



Optical properties of highly turbid shallow lakes with contrasting turbidity origins: The ecological and water management implications



G.L. Pérez ^{a,*}, L. Lagomarsino ^b, H.E. Zagarese ^b

^a Laboratorio de Fotobiología, Instituto de Investigaciones en Biodiversidad y Medio Ambiente (INIBIOMA, UNComahue-CONICET), R8400FRF, 8400 Bariloche, Río Negro, Argentina

^b Laboratorio de Ecología y Fotobiología Acuática, Instituto de Investigaciones Biotecnológicas, Instituto Tecnológico de Chascomús (IIB-INTECH CONICET), CC 164, 7130 Chascomús, Buenos Aires, Argentina

ARTICLE INFO

Article history:

Received 9 April 2013

Received in revised form

23 August 2013

Accepted 2 September 2013

Available online

Keywords:

Shallow turbid lakes

Water quality

Optical properties

Light penetration

Maximum colonization depth for SAV

Phytoplankton absorptive characteristics

Lake management

Ecological condition

ABSTRACT

A comprehensive optical study of three highly turbid shallow lakes was presented. The lakes contained very high concentrations of optically active substances [OASs] with clear differences in total suspended solid [TSS] composition among them. Lakes presented elevated values of total absorption [$a_t(\lambda)$] and scattering coefficients [$b(\lambda)$], which translated into extremely high light attenuation coefficients [$K_d(\text{PAR})$]. Differences among lakes in the estimation of $K_d(\text{PAR})$, using two typical estimators of light penetration (i.e., nephelometric turbidity [T_n] and Secchi disk [Z_{SD}]), were analysed. Kirk's optical model was used to model $K_d(\text{PAR})$ using inherent optical properties [IOPs]. Modelled values of $K_d(\text{PAR})$ agreed very well with those measured ($R^2 = 0.95$). In addition, optical properties and Kirk's model were used to determine water quality targets for restoring submerged aquatic vegetation [SAV]. Based on a minimum light requirement for SAV of 10%, results showed that only an integrative remediation action, considering substantial reduction of TSS and Chl *a* (95%), and CDOM (50%), must be contemplated to improve maximum colonization depth for SAV to values higher than 0.7 m. On the other hand, phytoplankton absorptive characteristics were also studied. In these lakes, phytoplankton showed different responses to the nature of light competition. Some of the variation in specific phytoplankton absorption [$a_{ph}^*(\lambda)$] was explained by differences in the ratio between unpigmented particulate absorption and phytoplankton absorption (up to $R^2 = 0.48$ for the blue band). Hydrologic optical results were discussed in terms of ecological and management implications.

© 2013 Elsevier Ltd. All rights reserved.

1. Introduction

Shallow lakes could exhibit alternative stable states with contrasting community structure (i.e., a clear-vegetated state vs. a turbid state) (Scheffer et al., 1993). Over the last decades, however, many lakes around the world have shifted from clear waters with abundant growth of macrophytes to turbid waters characterized by either blooms of Cyanobacteria or high sediment resuspension. Many lakes have shifted to a turbid state in response to progressive cultural eutrophication, and, once in a turbid state, they often exhibit resistance to change (e.g., Jeppesen et al., 1991; Kagalou et al., 2008; Hobbs et al., 2012). This scenario has promoted the study of shallow lakes within an ecological context with the ultimate goal of enhancing the efficiency of proactive strategies in

ecosystem management. Curiously, although the concept of light availability is at the core of current ecological theories on the functionality of shallow lakes, detailed optical studies of turbid lakes are scarce. For instance, several studies have routinely and uncritically used Secchi disk [Z_{SD}] and nephelometric turbidity [T_n] as estimators of light penetration in shallow lakes (e.g., Bayley and Prather, 2003; Jackson, 2003; Ibelings et al., 2007; Hargeby et al., 2007). The diffuse vertical light attenuation coefficient [$K_d(\text{PAR})$] is the intrinsic estimator of light penetration and is an apparent optical property [AOP]. Its value depends not only on the components in the water, but also on solar incidence angle, surface waves and cloud cover (Kirk, 1994a). Determination of $K_d(\text{PAR})$ is restricted to the availability of underwater light meters and weather conditions; therefore, proxies of light penetration are frequently needed.

Relationships between $K_d(\text{PAR})$ and both Z_{SD} and T_n have been rarely reported for highly turbid lakes. In addition, empirically derived relationships between $K_d(\text{PAR})$ and these estimators of light penetration have been shown to be site-specific (Effler, 1985;

* Corresponding author. Tel.: +54 294154330361.

E-mail addresses: perezgonzalouis@gmail.com, gperez@intech.gov.ar (G.L. Pérez).

Davies-Colley and Smith, 2001; Padial and Thomaz, 2008). Hence, using relationships developed for other systems could lead to inaccurate predictions of underwater light availability.

Underwater optical properties are very sensitive indicators of ecosystem changes and are therefore important to the interpretation of environmental signals (Tegler et al., 2001; Gallegos et al., 2005). Relationships between optical active substances [OASs], inherent optical properties [IOPs] and apparent optical properties have been studied in order to develop diagnostic tools capable of relating $K_d(\text{PAR})$ to the content of the water (e.g., V-Balogh et al., 2009), to set up a general expression to model light attenuation (e.g., Kirk, 1984) and to determine the main factors affecting temporal variability in water transparency (e.g., Gallegos et al., 2005; Pérez et al., 2011). Of significant relevance is the fact that light availability is an important factor controlling the distribution and abundance of submerged aquatic vegetation [SAV] (e.g., Schwarz et al., 2002; Caffrey et al., 2007). In shallow lakes where conditions favour development of SAV over large areas, there is potential for large-scale reductions of nutrients and phytoplankton concentration in the water column (Kufel and Kufel, 2002; Scheffer et al., 1994; Bakker et al., 2013). This occurs because SAV beds could stabilize sediments, sustain epiphyte that sequesters nutrients and lead to physical and chemical conditions that elicit removal of both particulate and soluble nutrients from the water column (Jeppesen et al., 1998). A maximum colonization depth of SAV [Z_{SAV}] is commonly estimated as: $Z_{\text{SAV}} = -\ln(\text{MLR}_{\text{SAV}})/K_d(\text{PAR})$, where MLR_{SAV} denotes the minimum light requirement for SAV growth. Areas of the lake that have water depth $\leq Z_{\text{SAV}}$ are potential sites for SAV development. Therefore, determination of target habitat requirements (i.e., minimal water quality levels) to improve light conditions for restoring SAV is critical to the management of shallow lakes. Water quality parameters were referred here as those substances, which are optically active, and therefore interact with light changing its spectral quantity and quality through the water column (e.g., TSS, Ash, T-Chl *a* and CDOM).

Additionally, the study of phytoplankton optical properties has important applications in the estimation of primary production [PP] by bio-optical models and in the retrieval of pigment biomass from remote sensing (e.g., Gordon and Morel, 1984; Strömbeck and Pierson, 2001; Marra et al., 2007). In this sense, detailed hydrologic optical characterization could provide valuable information on physico-chemical and biological processes of shallow turbid lakes, contributing significantly to assessing their ecological condition with important implications to water management.

The aim of this research was to perform a detailed optical characterization of three highly turbid Pampean shallow lakes with highly contrasting origins of turbidity and to evaluate and implement hydrologic optical results for the ecological and management needs. Here we report: (1) the relationships between $K_d(\text{PAR})$ and either Z_{SD} or T_n values; (2) the relationships between $K_d(\text{PAR})$ and IOPs, and the relationships between OASs concentration and IOPs; (3) the description of phytoplankton absorptive characteristics (i.e., specific absorption coefficients and spectral matching parameters) and (4) the use of optical properties and Kirk's model derived from Monte Carlo simulations (Kirk, 1984) to determine water quality targets for restoring SAV.

2. Material and methods

2.1. Study sites and sampling

Three neighbouring, highly turbid, permanent shallow lakes (i.e., Lake Chascomús, Lake San Jorge and Lake La Limpia) located in the Pampa Plain of Argentina (between 35° 36' S–35° 40' S and 57° 47' W–58° 02' W) were studied. A detailed characterisation of

these lakes and region is described in Allende et al. (2009) and Pérez et al. (2010).

Pampean lakes can be synthetically characterized as very shallow with a mean depth of approximately 2 m, polymictic, eutrophic or hypertrophic (Quirós et al., 2002). These lakes are subjected to a progressive eutrophication due to a combination of different human activities such as: land-use changes, increases in agriculture, fish introductions, drainage modifications, canalization and damming (Quirós et al., 2006). As a result, many Pampean lakes have shifted from a pristine, clear-vegetated state to a turbid state. For example, in Lake Chascomús decline of submerged vegetation (mainly *Potamogeton* sp.) occurred during years 1940–1980, probably due to the combined effects of flooding and human action (harvested and dredged). Nowadays, studied lakes present SAV only confined to small areas.

During the study, lakes were sampled and monitored throughout various seasons between 2008 and 2012. The collected sample size from each lake was: Lake Chascomús ($n = 21$), Lake San Jorge ($n = 15$) and Lake La Limpia ($n = 15$). Routine measurements of water temperature [T], pH (Orion pH-meter), conductivity (Hach conductimeter), and dissolved oxygen concentration (YSI 5000 Meter), were performed *in situ* (see notation in supplementary inline Table A). Secchi disk depth was measured with a standard 20 cm diameter, black and white disk. In Lake Chascomús, the water column depth [Z_{mix}] (at a gauging site) was also routinely measured during the study period. In Lake San Jorge and Lake La Limpia, Z_{mix} was determined sporadically. Water samples from each lake were collected directly from approximately 20 cm below the surface and transported to the laboratory in 10 L polypropylene containers for chemical, physical and optical determinations.

2.2. Nutrients

Total phosphorus [TP] (from unfiltered water samples) and total dissolved phosphorus [TDP] (from GF/F filtered water) were converted to soluble reactive phosphorus [SRP] after acid digestion with potassium persulfate. In turn, SRP was determined by using molybdate reactive phosphorus according to standard analytical procedures (APHA, 1998). Nitrate, nitrite and ammonia were estimated following APHA (1998) procedures. Organic nitrogen levels were determined by using the semi-micro-Kjeldahl method (APHA, 1998). Total nitrogen [TN] was estimated as the sum of nitrates, nitrites and organic nitrogen.

2.3. Optical active substances (optical water quality parameters)

Total suspended solids concentration [TSS] was determined by weighing the dried residue (60 °C) retained by the filtration of a water sample through pre-rinsed and pre-combusted (530 °C, 2 h) GF/F filters. Non-volatile particulate matter [Ash] was estimated by reweighing the GF/F filters after combustion at 530 °C for 3 h (APHA, 1998). Chlorophyll *a* concentration [Chl *a*] was measured by ion pairing reverse-phase HPLC (see Section 2.8.2). Because of the chemical complexity of chromophoric dissolved organic matter (CDOM), its concentration was expressed using the absorption coefficient at a reference wavelength, 440 nm (Kirk, 1994a; Zhang et al., 2007a) (see Section 2.5).

2.4. Apparent optical properties

Incident solar radiation was recorded with a GUV 511 radiometer (Biospherical Instruments, Inc.) located in Buenos Aires (~100 km northeast from Lake Chascomús). In addition, solar radiation was also recorded near the shore of Lake Chascomús, using an IL1700 radiometer (International Light).

Underwater vertical profiles of spectral (380–750 nm) downward irradiance [$E_d(\lambda)$] were performed using a calibrated USB2000 (Ocean Optics) spectroradiometer, which was attached to a fibre optic probe with a CC-3-UV-T cosine corrected diffuser. These measurements were performed around noon inside a black plastic container (50 × 50 × 40 cm) filled with freshly collected lake water. This procedure was adopted to increase the accuracy of the measurements by eliminating the noise from wave action observed in *in situ* profiles. The magnitude of error induced by waves is substantial and cannot be ignored when analysing highly turbid lakes, where light is attenuated to less than 1% within the first 20 cm. Analogous methodologies have been applied to solve similar issues (Belmont et al., 2007; V-Balogh et al., 2009). The spectral vertical diffuse attenuation coefficient was determined from the slope of the linear regression of the natural logarithm of $E_d(\lambda)$ vs. depth. Broadband $K_d(\text{PAR})$ was calculated in the same way by integrating $E_d(\lambda)$ from 400 to 700 nm for each depth. Light attenuation values, obtained with this procedure, had been validated by comparing the results against *in situ* determinations of $K_d(\lambda)$ performed on calm days (i.e., no wave action). A good agreement between these two sets of variables had been obtained. For $K_d(\text{PAR})$ the following linear relationship was obtained: $K_d(\text{PAR}) \text{ in situ} = 1.04K_d(\text{PAR}) - 1.97$; $n = 15$ ($R^2 = 0.96$; $p < 0.001$). The euphotic depth [$Z_{1\%}$], the depth at which PAR falls to 1% of its value just under the surface, was calculated as: $Z_{1\%} = 4.605/K_d(\text{PAR})$. The mean irradiance in the water column [$E_z \text{ mean}$] was estimated following Ferrero et al. (2006).

2.5. Inherent optical properties

2.5.1. CDOM absorption

Absorbance of CDOM was measured from filtered (0.22 μm) water samples. Measurements were performed in 0.01 m quartz cuvettes and compared against an ultrapure water blank using a Lambda 35 (PerkinElmer) spectrophotometer (from 380 to 750 nm, at 1 nm intervals). Values for each wavelength were corrected by null point correction subtracting the reading at 750 nm. The CDOM absorption coefficients [$a_g(\lambda)$] were then calculated following Kirk (1994a).

2.5.2. Particulate absorption

The absorption spectra from total particulate matter [$a_p(\lambda)$], unpigmented phytoplankton cell components, heterotrophic organisms detritus and minerals [$a_d(\lambda)$] (hereinafter absorption by unpigmented particles) and by phytoplankton pigments [$a_{ph}(\lambda)$] were determined by the quantitative filter technique [QFT] using the simple transmittance method. Measurements were made in a Lambda 35 (PerkinElmer) spectrophotometer (from 380 to 750 nm, at 1 nm intervals). Material was collected into 47 mm diameter GF/F filters according to NASA's optics protocols for absorption coefficient measurements (Mitchell et al., 2000). Absorption from unpigmented particles [$a_d(\lambda)$] was determined by using the extractive method following procedures set forth by Kishino et al. (1985). Readings of absorbance from total particles and unpigmented particles were checked to be lower than 0.4 (Cleveland and Weidemann, 1993). As standard procedure, a null point correction was set at 750 nm (Mitchell et al., 2000), where absorbance by the sample was assumed to be negligible and the readings in the near-infrared portion of the spectrum are considered as part of the scattering loss error. Particularly, for Lake La Limpia, the assumption of spurious absorption at infrared does not seem to hold, as systematically low values of the modelled $K_d(\lambda)$ were achieved with Kirk's model when the null point correction from 750 nm was applied to the measured values (see Section 2.6). For this lake the readings from 750 nm were considered as true absorption from

unpigmented particles. The same consideration was taken into account by Gallegos (1994) for turbid estuarine waters.

For all readings, absorbance from total particles and unpigmented particles was also corrected for the increase in path length caused by multiple scattering in the glass-fiber filter using the following equation (Cleveland and Weidemann, 1993):

$$A_{\text{susp}}(\lambda) = 0.378A_{\text{filter}}(\lambda) + 0.523A_{\text{filter}}(\lambda)^2 \quad (1)$$

where $A_{\text{susp}}(\lambda)$ is the path length corrected absorbance and $A_{\text{filter}}(\lambda)$ is alternatively the measured absorbance by total particulate matter or, after extraction, the absorbance by unpigmented particles.

The absorption coefficients for total particles and unpigmented particles were calculated as follows:

$$a_{p,d}(\lambda) = \frac{2.303A_{\text{susp}}(\lambda)}{(V/S)} \quad (2)$$

where 2.303 is the factor used to convert base 10 to a natural logarithm, V is the filtered volume and S is the filter clearance area.

Phytoplankton absorption coefficients were obtained by subtracting $a_d(\lambda)$ from $a_p(\lambda)$. The Chl *a* specific phytoplankton absorption coefficient [$a_{ph}^*(\lambda)$] was estimated as: $a_{ph}(\lambda)/T\text{-Chl } a$ (where $T\text{-Chl } a$ represents chlorophyll *a* + phaeophytin *a*). The absorption of particulate matter per unit of TSS mass [$a_p^m(\lambda)$] (hereinafter TSS mass specific absorption coefficient) was calculated as: $a_p(\lambda)/\text{TSS}$. The total absorption coefficient [$a_t(\lambda)$] was estimated as the sum of the absorption coefficients from particles, CDOM and pure water [$a_w(\lambda)$]. The absorption coefficients for pure water were taken from Pope and Fry (1997). Broadband absorption coefficients for PAR [i.e., $a_t(\text{PAR})$, $a_g(\text{PAR})$, $a_p(\text{PAR})$, $a_d(\text{PAR})$, $a_{ph}(\text{PAR})$ and $a_w(\text{PAR})$] were calculated as arithmetic averages within the 400–700 nm range. Phytoplankton absorption was studied specifically in the blue and red spectral regions, where $a_{ph}(\text{Blue})$ and $a_{ph}(\text{Red})$ represent the maximum values from the blue (between 430 and 444 nm) and red (between 670 and 680 nm) spectral regions. The effect of packaging on $a_{ph}^*(\lambda)$ was assessed by computing the dimensionless factor, denoted Q_a^* . Assuming a specific absorption coefficient for Chl *a* in a solution of 0.0207 $\text{m}^2 \text{mg}^{-1}$ at 675 nm, the dimensionless factor $Q_a^*(675)$ was estimated as: $a_{ph}^*(675)/0.0207$ after correcting $a_{ph}^*(675)$ for the possible presence of Chl *b* or divinyl Chl *b* (Bricaud et al., 1995).

2.5.3. Nephelometric turbidity and light scattering

Nephelometric turbidity, a proxy for light scattering, was measured with a bench-top 2100P turbidimeter (Hach) and calibrated against Formazin liquid standards (Hach). The spectral scattering coefficient [$b(\lambda)$] was calculated using T_n values derived from Gallegos (1994) with the following equation:

$$b(\lambda) = \left(\frac{550}{\lambda}\right) T_n \quad (3)$$

where the 550/ λ term introduces the inverse wavelength dependence of scattering coefficient suggested by Morel and Gentili (1991). The scattering coefficient per unit of TSS mass [$b^m(\lambda)$] (hereinafter TSS mass specific scattering coefficient) was calculated as: $b(\lambda)/\text{TSS}$. The broadband scattering coefficient for PAR [$b(\text{PAR})$] was calculated as arithmetic averages within the 400–700 nm.

2.6. Modelling of $K_d(\text{PAR})$ using Kirk's model

In a series of papers, Kirk (1981, 1984, 1994b) has used Monte Carlo computer simulations of the radiative transfer equation to estimate approximate algebraic expressions relating various AOPs to the IOPs.

One expression that is particularly useful because of its simplicity is the expression that denotes the average value of the vertical attenuation coefficient for downward irradiance in the euphotic zone as an explicit function of a , b , and μ_0 as follows (Kirk, 1991):

$$K_d(\text{PAR}) = \frac{1}{\mu_0} [a_t^2 + (g_1\mu_0 - g_2)a_t b]^0.5 \quad (4)$$

where μ_0 is the average cosine of the angle of the stream of photons just under the surface (calculated from the incident zenith angle using Snell's Law), g_1 and g_2 are numerical constants that vary with the volume scattering function used in the calculations, which with μ_0 specify the relative contribution of scattering to vertical attenuation. The spectral dependence of K_d , a_t and b in equation (4) has been omitted for clarity. The coefficients $g_1 = 0.425$ and $g_2 = 0.19$, estimated for water bodies by using the San Diego scattering phase function (Kirk, 1994a) were used and coefficients $a_t(\lambda)$ and $b(\lambda)$ were estimated to solve equation (4) in studied lakes. Broadband $K_d(\text{PAR})$ was then calculated by propagating the solar spectrum just below the surface, $E_d(0, \lambda)$, to a reference depth and numerically integrated over wavelength following Gallegos (1994). Finally, the relative contribution of scattering and absorption from dissolved and particulate fractions in the light attenuation mechanism were examined by calculating different optical conditions following procedures set forth by Belzile et al. (2002).

2.7. Determining habitat requirements for SAV

We began by evaluating the ability of Kirk's optical model to accurately estimate light attenuation from IOPs. Then the model was checked to see if it can consistently reproduce observed relationships between measured $K_d(\text{PAR})$ and measured relevant water quality parameters (i.e., TSS, Ash and T-Chl a) within the range of condition actually encountered in each lake. Subsequently, following Gallegos (1994, 2001), the model was used to investigate conditions not found in the sampling. The optical model allows the determination of concentration of water quality parameters that will result in a particular value of $K_d(\text{PAR})$ that permit survival of SAV at a particular stratum. The model is constructed in terms of IOPs, therefore obtained mean values of specific absorption and scattering coefficients were used to extrapolate IOPs from concentration of water quality parameters. We established Z_{SAV} values testing, in a simplified way, different management actions evaluating percentage reduction of mean values of water quality parameters as follows: (i) Reduction of T-Chl a ; (ii) Reduction of particulate matter (i.e., TSS with a proportional reduction of T-Chl a , such as a dilution process) and (iii) Reduction of TSS and T-Chl a with a fixed reduction of CDOM of 50%. Note that the alone reduction in T-Chl a by remediation actions entails a reduction in TSS by at least the amount of the dry weight of phytoplankton. Contribution of phytoplankton chlorophyll to TSS was estimated following Gallegos (2001). Maximum SAV colonization depth and its corresponded target habitat requirements (i.e., concentration of water quality parameters) were calculated with Kirk's model considering an SAV minimum light requirement of 10% of surface irradiance, following Canfield et al. (1985), Middelboe and Markager (1997). A fixed value of $\mu_0 = 0.87$ was used in all analysis.

2.8. Phytoplankton absorptive characteristics

2.8.1. Phytoplankton absorption and spectral matching parameters

The amount of light throughout the water column does not necessarily reflect the light that is absorbed by microalgae. In fact, light energy absorbed by phytoplankton depends on the spectral irradiance of their ambient light field and the spectral absorption

characteristics of its cells (Morel, 1978). Following procedures set forth by Markager and Vincent (2001), the spectral matching between these two sets of variables was evaluated. The absorption efficiency parameter $[A_e]$ and the effective absorption coefficient $[\hat{a}_{\text{ph}}]$ were calculated using the following equations:

$$A_e(Z) = \frac{\int_{400}^{700} E_d(Z, \lambda) a_{\text{ph}}(\lambda) d\lambda}{\left(\int_{400}^{700} E_d(Z, \lambda) d\lambda \right) \frac{\sum a_{\text{ph}}(\lambda)}{n}} \quad (5)$$

$$\hat{a}_{\text{ph}}(Z) = \frac{\int_{400}^{700} E_d(Z, \lambda) a_{\text{ph}}(\lambda) d\lambda}{\int_{400}^{700} E_d(Z, \lambda) d\lambda} \quad (6)$$

where $E_d(Z, \lambda)$ is the downward irradiance, at wavelength λ and depth Z , converted from energy units to quantum units ($\mu\text{mol photons m}^{-2} \text{ s}^{-1} \text{ nm}^{-1}$). The term n , in equation (5), refers to the number of phytoplankton absorbance measurements over the PAR range. The parameter \hat{a}_{ph} was expressed per unit of Chl a to obtain the specific effective absorption coefficient $[\hat{a}_{\text{ph}}^*]$.

2.8.2. Phytoplankton pigment composition

Phytoplankton pigments were estimated from samples (50–250 mL) collected by Whatman GF/F filters. The filters were immediately wrapped in aluminium foil and stored at -80°C . Pigments were extracted using 90% v/v aqueous acetone and then the extracts were cleared by centrifugation at 3000 rpm for 10 min. Pigment extracts were measured by ion pairing reverse-phase HPLC. The applied method is described in detail by Laurion et al. (2002). For this analysis, a Äkta basic chromatograph (Amersham, Buckinghamshire, UK), with a Phenomenex® Gemini C18 column ($250 \times 4.6 \text{ mm}$, $5 \mu\text{m}$), was used. Pigment identification and quantification, were made with standards from Sigma Inc. (Buchs, Switzerland) and from the International Agency for ^{14}C Determination. A few carotenoids, for which no standards were available, were identified based on published retention times [RT] and denoted as [carot (RT)]. The procedure used, however, did not allow the individualization of zeaxanthin and lutein, which coeluted as a single peak (referred to as Zea + Lut). The contribution of each pigment to the Zea + Lut concentration was calculated from the Lut/Chl b ratio reported by Guisande et al. (2008).

2.9. Statistical analysis

Linear regression (simple and multiple models) and correlation analyses were used to examine the relationships between the variables. The relationships between $K_d(\text{PAR})$ and Z_{SD}^{-1} were forced to intercept through the origin (0,0) following Koenings and Edmundson (1991). One-way ANOVA tests (using the Holm-Sidak method) were carried out to analyse differences in the mean values of OAS concentrations and optical properties among the studied lakes. Analyses of covariance (ANCOVA) were used to test the hypothesis, in which the regression parameters (i.e. slope and intercept) of optical properties differed significantly. Prior to each analysis, the Shapiro–Wilk Test and Spearman Rank Correlation were ran in order to test the data for normality and constant variance, respectively. Whenever the data did not conform, the values were transformed as

necessary, or nonparametric tests such as: Spearman Rank Order [R_s] for correlation studies and Kruskal–Wallis ANOVA on Ranks for ANOVA, were utilized. The regression determination coefficient [R^2], the regression slope and the relative root mean square error [RRMSE] were used to evaluate the performance of the retrieval model for estimating $K_d(\text{PAR})$ using Kirk's equation.

3. Results

3.1. Physicochemical characteristics and optical active substances

The three studied lakes presented high nutrient concentrations with mean values of TP ranging from 378 to 880 $\mu\text{g L}^{-1}$ and TN from 1103 to 2249 $\mu\text{g L}^{-1}$ (Table 1). Lake La Limpia showed a significant higher SRP concentration with a mean value of 582 $\mu\text{g L}^{-1}$ (ANOVA, $p < 0.001$).

In the three studied lakes the optical active substances were characterized by very high TSS concentrations with values ranging from 53 to 592 mg L^{-1} and mean values above 120 mg L^{-1} (Table 1). A significantly lower mean value for TSS was observed in Lake San Jorge (ANOVA, $p < 0.001$). Moreover, T-Chl a and Ash concentrations spanned a wide range among the studied lakes (Table 1). Significant differences in T-Chl a concentrations were observed among the studied lakes (ANOVA, $p < 0.001$). High values (above 70 $\mu\text{g L}^{-1}$) were observed in Lakes San Jorge and Chascomús, though Lake La Limpia was found to contain the lowest T-Chl a concentration (Table 1). Concerning Ash concentration, Lake San Jorge contained significant lower values (ANOVA, $p < 0.001$). Clear differences in the TSS composition were also observed between the studied lakes. Specifically, significant differences in T-Chl a /TSS ratios were observed (ANOVA, $p < 0.001$). The lowest values were observed in Lake La Limpia with a mean T-Chl a /TSS ratio of 0.26×10^{-3} , followed by Lake Chascomús and Lake San Jorge, which had means of 0.9×10^{-3} and 3.86×10^{-3} , respectively. Lake San Jorge was found to contain the lowest Ash/TSS ratio with a mean of 0.21 (ANOVA, $p < 0.001$). The mean Ash/TSS ratio was 0.65 in Lake Chascomús, while Lake La Limpia presented the highest mean Ash/TSS ratio of 0.85. CDOM concentration was also high in the three lakes with values of $a_g(440)$ ranging from 1.99 to 18.66 m^{-1} .

3.2. Underwater light filed in highly turbid lakes

3.2.1. Light attenuation and light penetration estimates

Typical spectral distributions of *in situ* underwater downwelling irradiance for the three studied lakes are depicted in Fig. 1. Profiles of $E_d(\lambda, Z)$ were normalized by the corresponding E_d maximum for

each depth in order to visualize spectral signatures throughout the euphotic zone. In these lakes, the downwelling flux decreased quickly within a few centimetres below the surface. The rapid attenuation at the short-wavelength end of the spectrum implies an almost complete removal of blue and green light within the first few centimetres (5–10 cm) (Fig. 1). At the euphotic depth (thick lines), the photosynthetically available flux consists exclusively of irradiances above 550 nm. Some differences were observed in spectral composition of E_d vs. depth between lake La Limpia and the other two lakes (Fig. 1).

The attenuation coefficients for PAR band were extremely high in all of the studied lakes, with values ranging from 9.7 to 47.9 m^{-1} . Mean values of $K_d(\text{PAR})$ were above 23 m^{-1} and showed little variations between the lakes. Although not significant, a slightly lower mean attenuation coefficient was registered in Lake La Limpia and a higher mean value in Lake San Jorge (Table 1). Euphotic depths, $Z_{1\%}$, ranged from 0.10 to 0.47 m, with a mean value about 0.23 m. Mean daily irradiances of the water column, $E_{z \text{ mean}}$, varied from 0.78 to 3.98 W m^{-2} .

Concerning spectral composition of light attenuation, important differences between the lakes were observed (Fig. 2). The three studied lakes presented maximum $K_d(\lambda)$ values in the blue spectral region (between 400 and 440 nm). Lake San Jorge, however, presented spectral shapes clearly influenced by phytoplankton absorption signatures. In contrast, Lake La Limpia showed an attenuation spectra characterized by decreasing values with increasing wavelengths. In this lake, a slight increase of attenuation in the red spectral region was occasionally observed (Fig. 2). Lake Chascomús presented an intermediate spectral light attenuation shape when compared to the other lakes.

Nephelometric turbidity was high, as could be expected given the elevated concentration of suspended solids. Values of T_n varied from 45 to 510 NTU, with mean values above 170 NTU (Table 1). Lakes San Jorge and La Limpia were found to have almost the same mean value for turbidity, while Lake Chascomús contained a slightly higher turbidity value (Table 1).

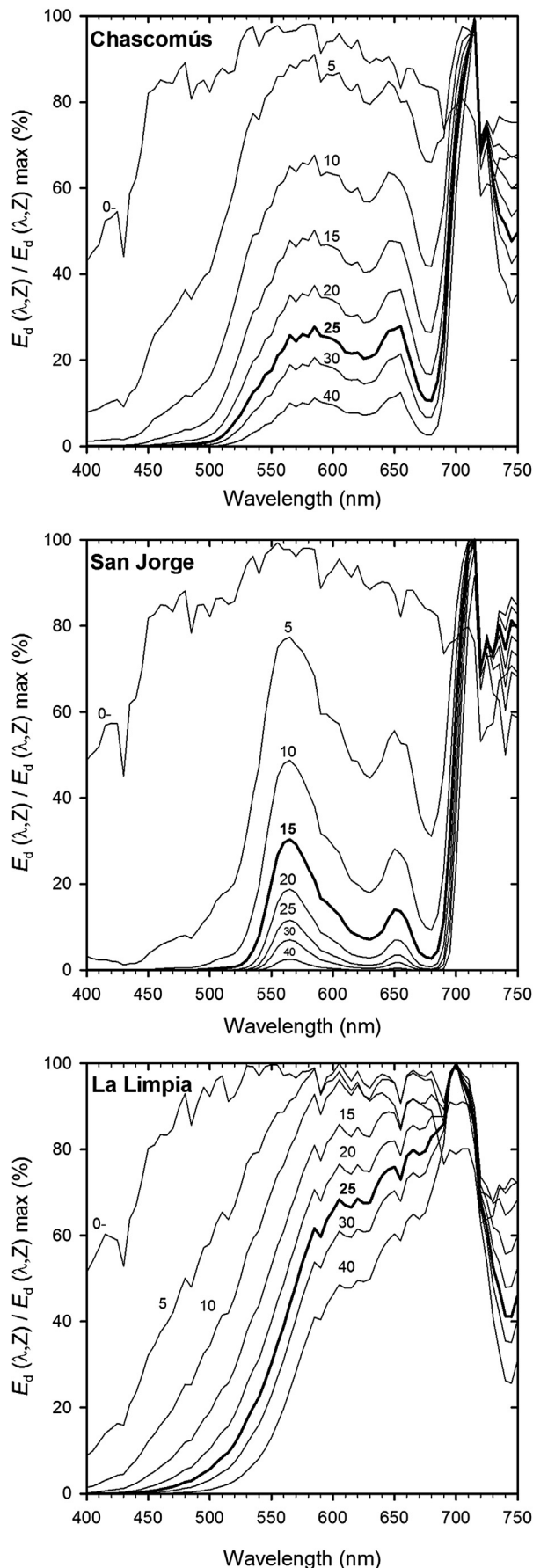
Measurements of the Secchi disk depth were all observed to be within a very narrow range, from 0.05 to 0.23 m, with a mean value below 0.12 m (Table 1). Although not significant, Lake Chascomús presented a slightly lower mean value for Z_{SD} , while a higher mean value was registered in Lake San Jorge (Table 1).

3.2.2. Relationships among $K_d(\text{PAR})$, OASs, T_n and Z_{SD}

For each of the studied lakes, differences in the TSS concentrations strongly explained the observed variation in $K_d(\text{PAR})$ (Table 2); however, when considering all of the lakes, the amount of

Table 1
Nutrient concentration, optical active substances (OASs) and light penetration proxies.

Lakes		TP ($\mu\text{g L}^{-1}$)	SRP ($\mu\text{g L}^{-1}$)	TN ($\mu\text{g L}^{-1}$)	TSS (mg L^{-1})	Ash (mg L^{-1})	Chl a ($\mu\text{g L}^{-1}$)	$K_d(\text{PAR})$ (m^{-1})	T_n (NTU)	Z_{SD} (m)
Chascomús	Mean	651.2	13.6	1103.8	264.1	174.6	196.5	25.1	237.3	0.09
	SD	(213.4)	(9.1)	(757.3)	(145.2)	(106.6)	(58.1)	(10.5)	(138.9)	(0.04)
	Min.	182.0	4.0	253.0	56.0	18.0	72.9	9.7	44.8	0.05
	Max.	1135.0	46.0	1838.0	592.0	398.0	300.1	47.9	509.0	0.20
	n	21	21	21	21	21	19	21	21	18
San Jorge	Mean	378.6	20.8	2249.3	122.4	32.7	482.3	29.2	173.0	0.11
	SD	(168.6)	(11.8)	(1041)	(63.5)	(32.5)	(305.8)	(12.1)	(93.2)	(0.05)
	Min.	198.0	8.0	840.0	53.0	7.0	202.8	10.6	63.1	0.05
	Max.	728.7	45.0	3438.0	300.0	127.0	1205.3	46.5	362.0	0.23
	n	15	15	15	15	15	14	15	15	14
La Limpia	Mean	880.7	582.4	1899.8	265.4	230.2	58.8	23.7	177.1	0.10
	SD	(255.3)	(119.1)	(1394.9)	(88.4)	(85.4)	(38.1)	(5.9)	(34.1)	(0.01)
	Min.	297.0	384.0	721.0	129.0	110.0	15.7	14.5	113.3	0.08
	Max.	1117.0	733.0	4905.0	502.0	465.0	117.1	32.5	229.0	0.14
	n	15	15	15	15	15	14	15	15	13



variation in light attenuation explained by the differences in TSS concentrations was lower [$K_d(\text{PAR}) = 0.058\text{TSS} + 13.01$; $n = 51$; $R^2 = 0.43$; $p < 0.001$]. When considering the contribution from other OASs to light attenuation, it was found that in Lake San Jorge the T-Chl a concentration, which is strongly correlated with TSS, explained a slightly higher variation in light attenuation than TSS (Table 2) ($R_s = 0.84$; $p < 0.001$). In Lake Chascomús, it was found that the Ash concentration explained 91% of the variation in $K_d(\text{PAR})$ and 71% of the variation by T-Chl a ; however, if T-Chl a is combined with TSS, their contribution was found to be not significant ($p = 0.21$). In Lake La Limpia, Ash explained the 76% of the variation in light attenuation and the contribution of T-Chl a was found to be not significant ($p = 0.38$). CDOM concentration, as $a_g(440)$, did not significantly explain the observed variation in $K_d(\text{PAR})$ in these lakes.

The nephelometric turbidity explained some of the observed variation in $K_d(\text{PAR})$. When considering all of the lakes, a significant linear relationship was found [$K_d(\text{PAR}) = 0.09T_n + 7.26$; $n = 51$; $R^2 = 0.83$; $p < 0.001$]. Individual lakes, however, presented a strong linear relationship between $K_d(\text{PAR})$ and turbidity, indicating little variation in optical attributes of TSS within each lake (Table 2, Fig. 3A). Values for R^2 were above 95% in both Lakes Chascomús and San Jorge and approximately 60% in Lake La Limpia. Among the studied lakes, dissimilarities in these relationships were observed indicating variable responses in $K_d(\text{PAR})$ with changes in turbidity (Table 2, Fig. 3). Significant differences in slopes and intercepts were found between Lake Chascomús and the other two lakes (ANCOVA, $p < 0.001$), but no significant differences were found between Lakes San Jorge and La Limpia (ANCOVA, $p < 0.053$).

The Secchi disk is commonly used as an estimator of $K_d(\text{PAR})$. When considering all of the studied lakes, differences in Z_{SD} explained much of the observed variation in $K_d(\text{PAR})$. In fact, a significant linear relationship was observed between $K_d(\text{PAR})$ and Z_{SD} [$K_d(\text{PAR}) = 2.18 Z_{SD}^{-1}$; $n = 45$; $R^2 = 0.74$; $p < 0.001$]. For each lake, significant variation in the $K_d(\text{PAR})$ was explained by changes in the reciprocal of the Z_{SD} readings (Fig. 3B, Table 2). Higher regression coefficient was obtained for Lake San Jorge ($R^2 = 0.89$), while a lowest regression coefficient was obtained for Lake La Limpia ($R^2 = 0.61$). No significant differences in regression slope among the studied lakes were observed (ANCOVA, $p = 0.17$) (Table 2).

3.3. Inherent optical properties

3.3.1. Absorption and scattering coefficients

The three studied lakes were found to contain very high values of total absorption coefficients for PAR, with values ranging from 5 to 27 m^{-1} and a mean value above 10 m^{-1} (Table 3). A higher mean value for $a_t(\text{PAR})$ was observed in Lake San Jorge, followed by Lake La Limpia. Lake Chascomús presented significantly lower values for $a_t(\text{PAR})$ when compared to Lake San Jorge (ANOVA, $p < 0.01$). Additionally, important differences in the contribution of different fractions (i.e. particles and CDOM) to the total light absorption were observed. The three studied lakes presented a dominance of absorption by suspended particles. In Lake San Jorge, phytoplankton absorption coefficients contributed the most to light absorption, with comparatively lower contributions from unpigmented particles and CDOM in decreasing order (Table 3, Fig. 4). In Lake Chascomús, the contributions of absorption from both phytoplankton and unpigmented particles were similar and dominant, followed by CDOM (Table 3, Fig. 4). Lake La Limpia showed to have the greatest

Fig. 1. In situ spectral downwelling irradiance in typical situations. For each depth the curve is normalized by its maximum. The actual depth of measurements is given on the figures. In thicker line irradiances at the bottom of euphotic depth.

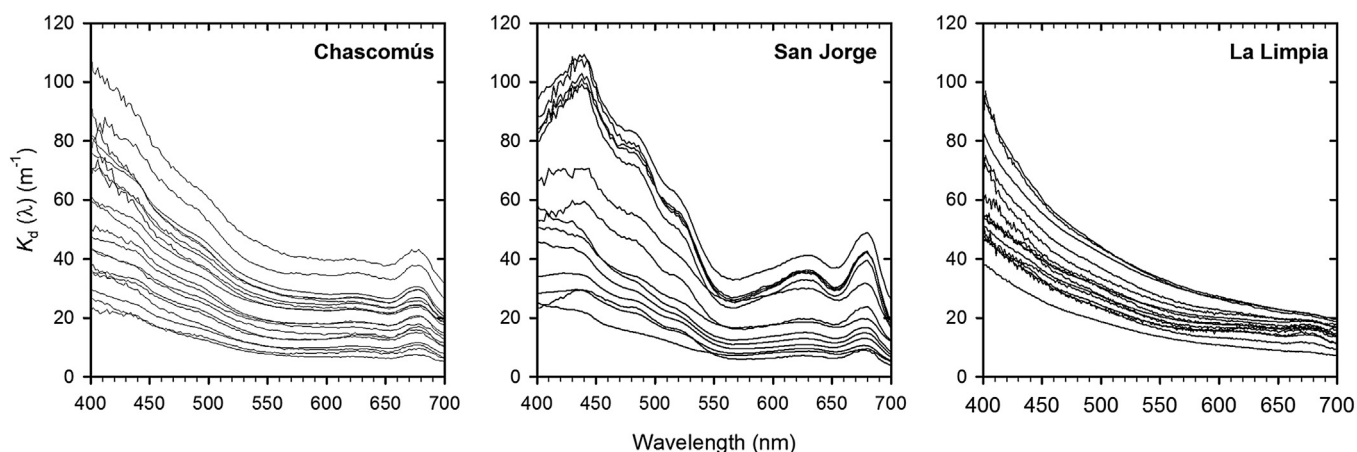


Fig. 2. Spectral vertical diffuse attenuation coefficients for each lake.

contribution from unpigmented particulate absorption; however, absorption from CDOM was also found to have significant importance (Table 3, Fig. 4).

Scattering coefficients for PAR were also found to be very high in all of the studied lakes, with values ranging from 46 to 520 m^{-1} and mean values above 175 m^{-1} (Table 3). Although not statistically significant, Lake Chascomús presented a higher mean value of $b(\text{PAR})$, while Lakes San Jorge and La Limpia showed similar and comparatively lower mean values (Table 3). The relative contribution of absorption and scattering processes in each lake yielded significant differences when analysing the b/a_t ratios. In all lakes, the b/a_t ratio for PAR band presented high values, ranging from 13 to 43, with a mean ratio above 16 (Table 3). The highest b/a_t ratios for PAR were observed in Lake Chascomús, followed by Lake La Limpia. Lake San Jorge presented significantly lower b/a_t ratios for PAR when compared to Lake Chascomús (ANOVA, $p < 0.01$). If $b(\text{PAR})/a_t(\text{min})$ ratio was considered [where $a_t(\text{min})$ stands for the minimum value of $a_t(\lambda)$ between 400 and 700 nm], higher mean b/a_t ratios were obtained. Lake Chascomús presented a mean ratio of 86, followed by Lake San Jorge, with a mean of 61, and Lake La Limpia with a mean of 59.

Clear differences were also observed in the TSS mass specific absorption and scattering coefficients in the PAR band (Table 3). Lake San Jorge presented significantly higher values for $a_p^m(\text{PAR})$ when compared to Lakes La Limpia and Chascomús (ANOVA, $p < 0.001$). Values of $b^m(\text{PAR})$ were significantly different among all of the studied lakes (ANOVA, $p < 0.001$). Higher mean values for $b^m(\text{PAR})$ were obtained for Lake San Jorge, followed by Lake Chascomús and then Lake La Limpia (Table 3). Differences in $a_p^m(\text{PAR})$ and $b^m(\text{PAR})$ were caused by particulate matter composition. When considering all of the studied lakes, values for $a_p^m(\text{PAR})$ were found to significant correlate with the T-Chl a/TSS ($R_s = 0.67$, $p < 0.001$)

and Ash/TSS ratios ($R_s = -0.66$, $p < 0.001$). This lead to an increase in absorption per unit of TSS with either an increase in T-Chl a content of TSS or a decrease in Ash content. Similarly, the $b^m(\text{PAR})$ coefficients were also found to have a strong correlation with the T-Chl a/TSS ($R = 0.89$, $p < 0.001$) and Ash/TSS ratios ($R_s = -0.82$, $p < 0.001$), which denoted an increase of scattering per unit of TSS with increases in the concentration of organic particles.

3.3.2. Relationships between IOPs and light attenuation

A good agreement between measured and modelled values of $K_d(\lambda)$ was obtained with Kirk's model (equation (4)), which implies that, the overall magnitudes and spectral shapes were well predicted. When taking into account the three studied lakes, values for the modelled $K_d(\text{PAR})$ agreed very well with the measured ones ($R^2 = 0.95$; $n = 50$; $p < 0.001$), resulting in a near 1:1 relationship (regression slope 0.95 ± 0.03) and an RRMSE of 11.7% (Fig. 5). For each lake, the relationship between the measured and modelled $K_d(\text{PAR})$ values yielded R^2 values above 0.94 and RRMSE values below 15%. The model, however, tended to underestimate $K_d(\lambda)$ values, at the red-end spectral region (around 700 nm), with an overall mean of 19%.

When considering the relative contribution of IOPs to light attenuation, on average, the three lakes were found to have an important contribution from particulate absorption (between 37% and 50%) and scattering (between 39% and 52%) (see supplementary inline Fig. A). Light scattering increased attenuation by an average of 92%, when compared to what could have been expected from only absorption processes. Significant differences in phytoplankton absorption and unpigmented particulate absorption contribution to $K_d(\text{PAR})$ were observed among the studied lakes (ANOVA, $p < 0.001$). Lake La Limpia was found to contain slightly higher contribution from CDOM when compared to the other two

Table 2

Linear regression models for predicting $K_d(\text{PAR})$ from nephelometric turbidity, Secchi disk and OASs concentration.

Lakes	Light penetration proxies	Optical active substances
Chascomús	$K_d(\text{PAR}) = 7.8 \times 10^{-2} T_n + 6.93$ ($R = 0.96$; $n = 21$; $p < 0.001$) $K_d(\text{PAR}) = 2.01 Z_{SD}^{-1}$ ($R^2 = 0.74$; $n = 18$; $p < 0.001$)	$K_d(\text{PAR}) = 7.7 \times 10^{-2} \text{TSS} + 5.29$ ($R^2 = 0.95$; $n = 21$; $p < 0.001$) $K_d(\text{PAR}) = 0.10 \text{Ash} + 7.98$ ($R^2 = 0.91$; $n = 21$; $p < 0.001$) $K_d(\text{PAR}) = 0.15 \text{T-Chl } a - 4.82$ ($R^2 = 0.71$; $n = 19$; $p < 0.001$)
San Jorge	$K_d(\text{PAR}) = 0.13 T_n + 2.30$ ($R^2 = 0.97$; $n = 15$; $p < 0.001$) $K_d(\text{PAR}) = 2.22 Z_{SD}^{-1}$ ($R^2 = 0.89$; $n = 14$; $p < 0.001$)	$K_d(\text{PAR}) = 0.16 \text{TSS} + 6.12$ ($R^2 = 0.80$; $n = 15$; $p < 0.001$) $K_d(\text{PAR}) = 3.3 \times 10^{-2} \text{T-Chl } a + 10.4$ ($R^2 = 0.81$; $n = 14$; $p < 0.001$)
La Limpia	$K_d(\text{PAR}) = 0.12 T_n + 2.40$ ($R^2 = 0.61$; $n = 15$; $p < 0.001$) $K_d(\text{PAR}) = 2.48 Z_{SD}^{-1}$ ($R^2 = 0.61$; $n = 13$; $p < 0.005$)	$K_d(\text{PAR}) = 7.6 \times 10^{-2} \text{TSS} + 3.63$ ($R^2 = 0.79$; $n = 15$; $p < 0.001$) $K_d(\text{PAR}) = 7.7 \times 10^{-2} \text{Ash} + 6.34$ ($R^2 = 0.76$; $n = 15$; $p < 0.001$)

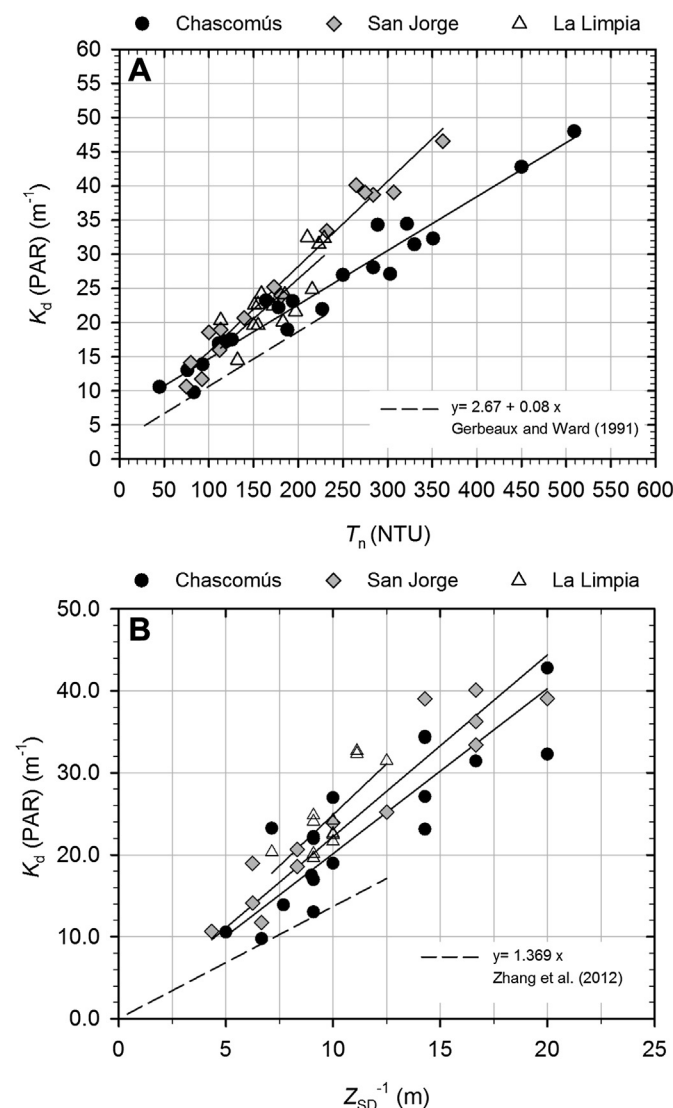


Fig. 3. (A) Relationship between $K_d(\text{PAR})$ and nephelometric turbidity found for each lake. The relationship obtained by Gerbeaux and Ward (1991) is shown for comparison. (B) Relationship between $K_d(\text{PAR})$ and the reciprocal of Secchi disk depth found for each lake. The relationship obtained by Zhang et al. (2012) is shown for comparison.

Table 3
Inherent optical properties and specific coefficients of light absorption and scattering.

Lakes		$a_t(\text{PAR})$ (m ⁻¹)	$a_g(\text{PAR})$ (m ⁻¹)	$a_d(\text{PAR})$ (m ⁻¹)	$a_{ph}(\text{PAR})$ (m ⁻¹)	$b(\text{PAR})$ (m ⁻¹)	b/a_t (d.l.)	$a_p^m(\text{PAR})$ (m ² g TSS ⁻¹)	$a_{ph}^*(\text{PAR})$ (m ² mg T-Chl a ⁻¹)	$b^m(\text{PAR})$ (m ² g TSS ⁻¹)
Chascomús	Mean	10.53	1.93	4.87	3.58	229.52	27.84	0.036	0.019	0.905
	SD	(4.64)	(0.66)	(2.84)	(1.24)	(132.68)	(8.12)	(0.008)	(0.002)	(0.075)
	Min.	5.08	1.05	1.14	1.45	45.97	12.93	0.023	0.013	0.754
	Max.	21.19	3.66	10.62	6.12	522.31	43.29	0.054	0.022	1.066
	n	20	20	21	21	21	20	21	19	21
San Jorge	Mean	18.73	2.76	2.91	12.92	177.57	16.51	0.105	0.021	1.430
	SD	(8.01)	(0.91)	(0.62)	(6.81)	(95.60)	(1.89)	(0.018)	(0.004)	(0.211)
	Min.	7.26	1.24	1.11	4.02	64.75	14.26	0.078	0.016	0.962
	Max.	27.21	5.10	3.25	21.66	371.46	20.33	0.140	0.029	1.892
	n	15	15	15	15	15	15	15	14	15
La Limpia	Mean	12.96	3.82	7.94	1.05	189.24	21.99	0.035	0.016	0.736
	SD	(4.99)	(3.31)	(2.54)	(0.78)	(45.98)	7.34	(0.008)	(0.004)	(0.108)
	Min.	6.31	0.80	2.93	0.20	116.22	13.49	0.024	0.009	0.617
	Max.	22.15	9.66	11.74	2.40	309.90	35.06	0.056	0.021	0.930
	n	15	15	15	15	15	15	15	14	15

Note: d.l. (Dimensionless).

lakes. When considering the scattering contribution to $K_d(\text{PAR})$, Lake Chascomús was observed to have a significantly higher contribution when compared to Lake San Jorge (ANOVA, $p < 0.001$).

3.3.3. SAV maximum depth of colonization and water quality requirements

Only a radical reduction of concentration of water quality parameters would increase maximum depth of colonization of SAV to promising values (Table 4). Values of Z_{SAV} between 0.5 and 1 m represent important areas of study shallow lakes. Values lower than 0.5 m are subjected to seasonal variation of water level resulting in physical stress for macrophytes thrive. Considering only the reduction of T-Chl a , even a decrease of 99% in mean values would not increase Z_{SAV} to values larger than 0.5 m. Lake San Jorge showed the higher increase in transparency translated in a Z_{SAV} of 0.32 m (Table 4). If a reduction of TSS with proportional reduction of T-Chl a is evaluated, 95% of reduction (i.e., $\text{TSS} < 13.3 \text{ mg L}^{-1}$ and $\text{T-Chl } a < 24 \mu\text{g L}^{-1}$) would elicit an increase of Z_{SAV} near or higher 0.5 m (Table 4). Studied lakes were observed to have high CDOM absorption values that represent an important background light attenuation. Considering only CDOM and pure water absorption (i.e., without absorption and scattering by particles), Z_{SAV} values would be 1.10, 0.87 and 0.65 m for Lakes Chascomús, San Jorge and La Limpia respectively. Therefore, evaluating a fixed CDOM reduction of 50%, in addition to a 95% of reduction in TSS and T-Chl a , would elicit values of $Z_{\text{SAV}} \geq 0.7 \text{ m}$ in the three lakes (Table 4).

3.3.4. Phytoplankton absorptive characteristics and pigment composition

Specific phytoplankton absorption revealed differences in amplitude and spectral shape among the studied lakes (Fig. 6). Values of $a_{ph}^*(\text{PAR})$ varied from 0.009 to 0.029 m² mg T-Chl a⁻¹ (Table 5), with significantly higher values in Lake San Jorge when compared to Lake La Limpia (ANOVA, $p < 0.001$). Values of $a_{ph}^*(\text{Blue})$ varied from 0.020 to 0.068 m² mg T-Chl a⁻¹ (Table 5), with significantly higher values in Lake San Jorge when compared to the other two lakes (ANOVA, $p < 0.001$). In the red region, values of $a_{ph}^*(\text{Red})$ varied from 0.009 to 0.024 m² mg T-Chl a⁻¹ (Table 5), with significantly higher values in Lake Chascomús when compared to Lake La Limpia (ANOVA, $p < 0.005$). Regarding the spectral shape, the ratio between $a_{ph}^*(\text{Blue})/a_{ph}^*(\text{Red})$ varied from 1.46 to 3.06. When compared to the other two lakes, Lake San Jorge was found to contain significantly higher $a_{ph}^*(\text{Blue})/a_{ph}^*(\text{Red})$ ratios with a mean ratio of 2.83 ± 0.17 (ANOVA, $p < 0.001$). Additionally,

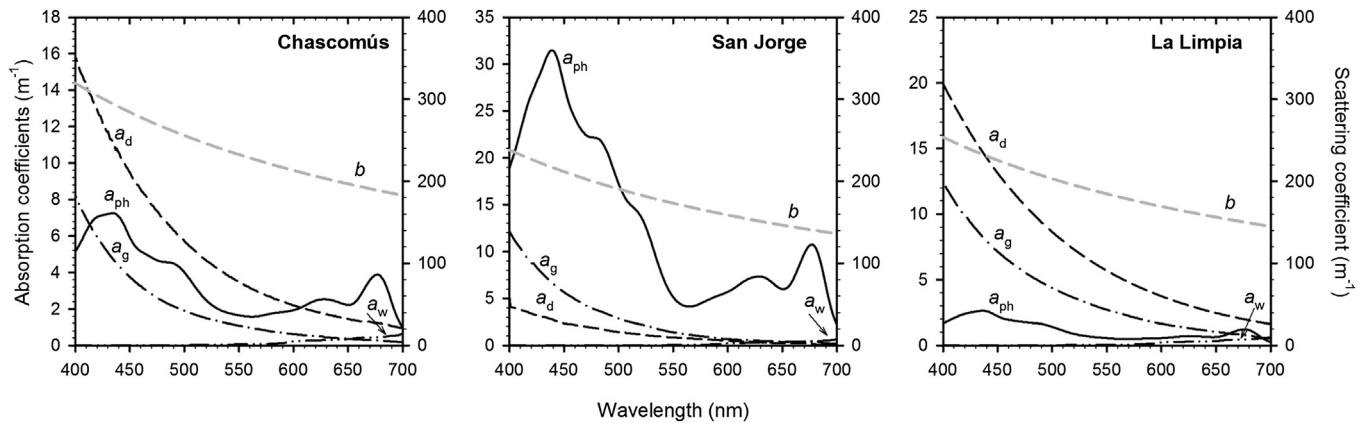


Fig. 4. Mean values of absorption and scattering coefficients. Note the different y-axis scales.

in this lake, $a_{ph}^*(\lambda)$ showed a secondary peak near 515 nm, which was not observed in Lakes Chascomús and La Limpia (Fig. 6).

When assessing the effects of external and internal factors on the variation in specific phytoplankton absorptions, it was found that differences in the ratio between $a_d(\lambda)/a_{ph}(\lambda)$ explained some of these observed variations. A significant negative linear relationship was found between $a_{ph}^*(\text{Blue})$ and the log of the ratio between unpigmented particulate absorption and phytoplankton absorption in the blue band [$a_d(\text{Blue})/a_{ph}(\text{Blue})$] ($R^2 = 0.48$; $p < 0.001$). This trend was also observed for $a_{ph}^*(\text{PAR})$ ($R^2 = 0.44$; $p < 0.001$) (Table 6).

Differences in specific phytoplankton absorption were also related to the pigment composition of different assemblages among the lakes. The phytoplanktonic accessory pigment concentrations are depicted in supplementary inline Table B. In Lake Chascomús, the composition of accessory pigments were dominated by Zeax, Lut, Fucox, Chl *b*, and Diato (in decreasing order), which together accounted for more than 70% of the total accessory pigment concentration [TAP]. These indicated that the phytoplankton community mainly consisted of Cyanobacteria, Chlorophytes and either Bacillariophytes or Chrysophytes. Lake San Jorge was found to have a dominance of pigments that are typically diagnostic of Cyanobacteria dominated phytoplankton (Zeax, Myxo-like carotenoid and Oscil). The unknown carotenoid [carot (19.5)] correlated well

with the Zeax concentration ($R = 0.71$, $p < 0.001$). Finally, in Lake La Limpia pigments were dominated by Lut, Chl *b*, Diato and Viola, which together accounted for more than 80% of the TAP concentration. In this lake, Chlorophytes and either Bacillariophytes or Chrysophytes would mainly constitute the phytoplankton community. In addition, the determination of small concentrations of Allo also indicates the presence of Chryptophytes.

When evaluating the effects of pigment composition on $a_{ph}^*(\lambda)$ for all three of the studied lakes, the differences in TAP/T-Chl *a* explained some of the observed variation in $a_{ph}^*(\text{blue})$ ($R^2 = 0.41$, $p < 0.001$) (Table 6). On the other hand, specific phytoplankton absorption in the red band [$a_{ph}^*(\text{Red})$], was found to be influenced primarily by pigment packaging. The dimensionless factor $Q_a^*(675)$ revealed mean values of 0.50, 0.48 and 0.43 for Lakes Chascomús, San Jorge and La Limpia, respectively. Although not significant ($p = 0.08$), Lake La Limpia showed a higher package effect when compared to the other studied lakes, which decreased absorption coefficients by 57% on average. The presence of the overlapping absorption band from Chl *b* can also contribute to the variation in $a_{ph}^*(\text{Red})$. In Lake Chascomús, differences in the Chl *b*/T-Chl *a* ratio explained some of the observed variation in $a_{ph}^*(\text{Red})$ ($R^2 = 0.47$, $p < 0.001$). In this lake, Chl *b* counteracts the absorption flattening due to T-Chl *a* packaging.

Light energy absorbed by phytoplankton, which was assessed by the absorption efficiency parameter [A_e] and the specific effective absorption coefficient [\hat{a}_{ph}^*], revealed differences between each of the studied lakes (Table 5). The three lakes presented A_e values lower than 1, indicating that the euphotic zones were dominated by spectral irradiances rich in wavelengths that are poorly absorbed by phytoplankton cells. Lake San Jorge showed a higher decrease in both A_e and \hat{a}_{ph}^* throughout the euphotic zone. This lake also was found to contain relatively lower values for A_e when compared to the other two lakes from and beyond the middle of euphotic zone (ANOVA, $p < 0.001$) (see supplementary inline Fig. B).

4. Discussion

4.1. Optical characteristics of highly turbid lakes: modelling and estimation of diffuse light attenuation

The three studied Pampean lakes are exceptionally turbid and optically complex water bodies. In the past, very few studies have reported comparable values of both OASs concentrations and optical properties in lentic ecosystems. Waters of comparable turbidity and complexity are mainly represented by highly turbid estuaries (e.g., Gallegos, 1994, 2001) and some other shallow lakes

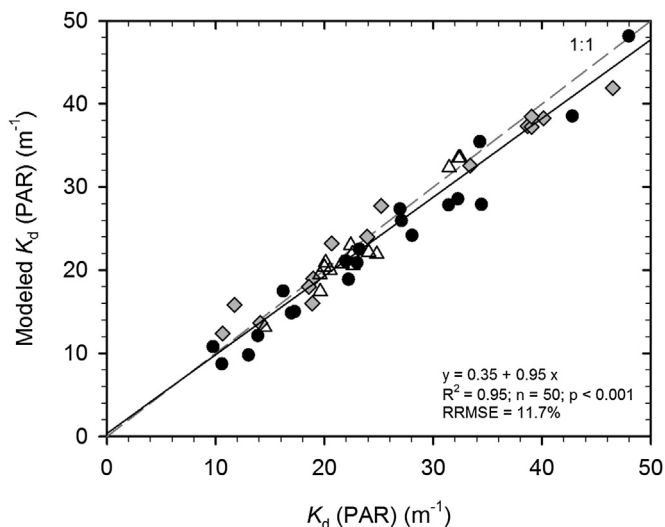


Fig. 5. Relationship between measured and modelled $K_d(\text{PAR})$.

Table 4

Maximum depth of SAV colonization in relationship with target reduction of water quality components resolved with Kirk's optical model.

Optical water quality conditions (evaluating management action)			Chascomús	San Jorge	La Limpia
			Maximum depth of SAV colonization (m)		
T-Chl a reduction	Percentage reduction	75%	0.14	0.20	0.11
		95%	0.15	0.29	0.12
		99%	0.16	0.32	0.12
TSS and T-Chl a reduction		75%	0.30	0.25	0.26
		95%	0.68	0.56	0.47
		99%	0.99	0.79	0.58
TSS, T-Chl a , and CDOM reduction		75%	0.34	0.28	0.32
		95%	0.93	0.78	0.70
		99%	1.60	1.29	0.99

Note: refer to [Material and methods](#) (Section 2.7) to description of tested management actions and optical model considerations.

around the world (e.g., [Nolen et al., 1985](#); [Gerbeaux and Ward, 1991](#); [Zhang et al., 2007b](#); [V-Balogh et al., 2009](#)).

By performing a detailed optical characterization of Pampean lakes, the relationships between AOPs and IOPs could be analysed. In this research, it can be pointed out that values of $K_d(\lambda)$ obtained by using Kirk's model revealed a strong agreement with measured attenuation coefficients. Kirk's equation has been used to calculate $K_d(\lambda)$ in diverse aquatic ecosystems, but its applicability in highly turbid waters has been only explored and supported by predictions from the Monte Carlo procedure ([Kirk, 1994b](#)). The empirical results from this research reveal that Kirk's equation may successfully be used to model $K_d(\text{PAR})$ in highly turbid waters with elevated ratios of scattering and absorption coefficients [mean values of $b(\text{PAR})/a_t(\text{min})$ above 59]. Underwater light (quantity and spectral composition) is of great importance to the functioning of shallow lakes; therefore an accurate and detailed description of light attenuation is essential to environmental management and ecological studies. Even if Kirk's model could be considered too complex for routine use in the water management community (e.g., when required the prediction of light attenuation using high-frequency data set), it can provide high accuracy in the estimation of $K_d(\text{PAR})$ in either turbid lakes with important spatial differences in optical properties or in studies encompassing lakes with contrasting origins of turbidity. Additionally, Kirk's model could be used by managers to rank the importance of reducing different attenuating components and, as was discussed below, to calculate target water quality conditions either to restore SAV (by

recolonization or planting) or to protect them (e.g., conservation of protected areas).

Some uncertainties, however, regarding modelled $K_d(\lambda)$ values in the red end of the spectra must be taken into account. An important source of error in modelling $K_d(\lambda)$ in turbid waters may be associated with the implementation of the null point correction for scattering error. In field samples, especially those including mineral and detrital particles, ignoring true absorption at the red end of the spectra results in an underestimation of $a_p(\lambda)$ ([Tassan and Ferrari, 1998](#); [Mitchell et al., 2000](#)). The implementation of the transmittance-reflectance method ([Tassan and Ferrari, 1995](#)) in turbid waters can significantly improve the reduction of errors in the determination of $a_p(\lambda)$.

The need for useful diagnostic tool for managers has led to the use of bench top instruments or simple, inexpensive measurements used for the estimation of light penetration. The simultaneous need for precision and functionality, however, usually presents conflicting requirements. For instance, nephelometric turbidity is often used as a rough estimator of TSS and water clarity ([Davies-Colley and Smith, 2001](#); [Chanson et al., 2008](#)). This, nevertheless, is actually a measurement of side scattering at 90° and therefore a proxy for light scattering. When considering all data sets, the differences in T_n were found to explain the 83% of the variation in $K_d(\text{PAR})$. This relationship emphasizes the importance of scattering and the optical attributes of TSS in the determination of light attenuation in the studied lakes. Similar regression results were recorded by [Gerbeaux and Ward \(1991\)](#) for the large and eutrophic Lake Ellesmere (see [Fig. 3A](#)). In contrast, if individual Pampean lakes were considered, significant relationship differences were found. The determination of IOPs allowed for the explanation of the differences observed between nephelometric turbidity and light attenuation coefficients. At similar values of T_n , and therefore alike $b(\text{PAR})$ coefficients, Lake Chascomús presented lower values for total absorption, which elicited higher b/a_t ratios translated into lower values of $K_d(\text{PAR})$ (maximum difference around 30%) ([Fig. 3A](#)). Lake San Jorge, however, when compared to Lake Chascomús, presented higher values of $K_d(\text{PAR})$ per unit of T_n due to its higher values for total absorption that translated in lower b/a_t ratios. Furthermore, Lake La Limpia presented a more variable relationship. When compared to the other two lakes, this pattern can be explained by its higher variance in CDOM absorption. The differences in b/a_t ratios among lakes were mainly determined by differences in TSS specific absorption and scattering coefficients, related to the particulate matter composition.

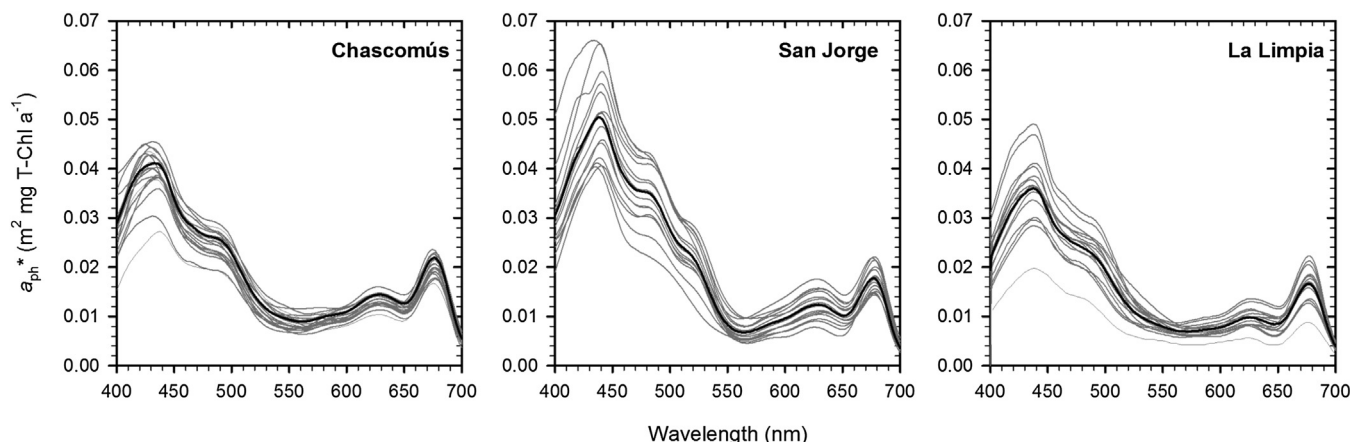


Fig. 6. Specific phytoplankton absorption coefficients. In thicker line mean $a_{ph}^*(\lambda)$ values.

Table 5
Phytoplankton specific absorption coefficients and spectral matching parameters.

Lakes		$a_{ph}^{*}(PAR)$ (m ² mg T-Chl a ⁻¹)	$a_{ph}^{*}(Blue)$ (m ² mg T-Chl a ⁻¹)	$a_{ph}^{*}(Red)$ (m ² mg T-Chl a ⁻¹)	$A_e(E_d - 0)$ (Dimensionless)	$A_e(E_d 50\%)$ (Dimensionless)	$A_e(E_d 1\%)$ (Dimensionless)	$\hat{a}_{ph}^{*}(E_d - 0)$ (m ² mg T-Chl a ⁻¹)	$\hat{a}_{ph}^{*}(E_d 50\%)$ (m ² mg T-Chl a ⁻¹)	$\hat{a}_{ph}^{*}(E_d 1\%)$ (m ² mg T-Chl a ⁻¹)
Chascomús	Mean	0.019	0.039	0.021	0.903	0.831	0.681	0.017	0.015	0.013
	SD	(0.002)	(0.005)	(0.002)	(0.039)	(0.045)	(0.056)	(0.002)	(0.002)	(0.002)
	Min.	0.013	0.027	0.018	0.841	0.743	0.586	0.012	0.011	0.009
	Max.	0.022	0.045	0.024	1.020	0.901	0.787	0.020	0.018	0.015
	n	19	19	19	21	21	21	19	19	19
San Jorge	Mean	0.021	0.050	0.018	0.856	0.680	0.431	0.020	0.016	0.010
	SD	(0.004)	(0.009)	(0.003)	(0.036)	(0.043)	(0.054)	(0.005)	(0.003)	(0.002)
	Min.	0.016	0.040	0.014	0.792	0.619	0.341	0.014	0.012	0.007
	Max.	0.029	0.068	0.022	0.904	0.741	0.512	0.031	0.022	0.014
	n	14	14	14	15	15	15	14	14	14
La Limpia	Mean	0.016	0.036	0.017	0.088	0.776	0.615	0.015	0.013	0.011
	SD	(0.004)	(0.009)	(0.004)	(0.021)	(0.019)	(0.011)	(0.002)	(0.002)	(0.001)
	Min.	0.009	0.020	0.009	0.856	0.752	0.605	0.012	0.011	0.008
	Max.	0.021	0.049	0.022	0.910	0.806	0.637	0.018	0.016	0.013
	n	14	14	14	15	15	15	14	14	14

Note: ($E_d - 0$) is the solar irradiance spectrum just below the surface.**Table 6**Linear regression models explaining variation in a_{ph}^{*} .

Independent variables	Dependent variables	Slope	Intercept	R ²	p	n
Log[$a_d(Blue)/a_{ph}(Blue)$]	$a_{ph}^{*}(Blue)$	-0.0102	0.042	0.476	<0.001	47
Log[$a_d(PAR)/a_{ph}(PAR)$]	$a_{ph}^{*}(PAR)$	-0.0035	0.018	0.437	<0.001	47
TAP/T-Chl a	$a_{ph}^{*}(Blue)$	0.023	0.024	0.410	<0.001	47

The Secchi disc was thought to have higher environmental relevance than turbidity, since it is a measurement of visual water clarity; however, a more variable overall correlation between Z_{SD}^{-1} and $K_d(PAR)$ was observed for studied Pampean lakes. Values of Z_{SD} explained lower variation in light attenuation when compared to turbidity (i.e., 74%). Additionally, a linear regression slope of 2.18 was obtained, which is considerably larger than the widely used factor of 1.7 (Poole and Atkins, 1929). This obtained factor is also larger than the value of 1.37 obtained by Zhang et al. (2012) for turbid Lake Taihu. Padial and Thomaz (2008), however, have reported high $K_d(PAR) \times Z_{SD}$ values in heterogeneous, neotropical waters with factors ranging from 1.83 to 2.55 (mean of 2.26). Koenings and Edmundson (1991) found that variation in $K_d(PAR) \times Z_{SD}$ was explained by lake-specific optical characteristics, making the factor increase with colour and decrease with turbidity. Nevertheless, the use of different factors in relation to water classification (i.e., clear, coloured and turbid lakes) must be taken with care, as the optical properties of a water body have continuous rather than discrete characteristics (Padial and Thomaz, 2008). The observed relationship between $K_d(PAR)$ and Z_{SD} in Pampean lakes (i.e., variable overall correlation, elevated factors, and no significant differences between the studied lakes) could be related to the singular optical characteristics found in these lakes, which caused the findings to expand beyond the previously identified range of this relationship for highly turbid waters (Zhang et al., 2012) (see Fig. 3B). Additional research will be needed to elucidate observed relationships between $K_d(PAR)$ and Z_{SD} in terms of differences in absorption and scattering coefficients among lakes and possible measurement errors caused by narrowest Z_{SD} values.

Even if good general relationships between $K_d(PAR)$ and light penetration estimates were found, observed differences among lakes should be pondered. To give an example of appreciable differences caused by the application of either generalised factors or lake-specific relationships, consider the use of the factor 1.7 to calculate $K_d(PAR)$ from mean Z_{SD} value in Lake Chascomús and the relationship between $K_d(PAR)$ and T_n , obtained for this lake to be used in Lake San Jorge. It yields a 31 and 25% of differences in the estimation of mean $K_d(PAR)$ values for Chascomús and San Jorge respectively. These differences may result in imprecise estimates of key parameters, which have $K_d(PAR)$ as input, used in water management, restoration processes and ecosystem monitoring (e.g., mean water column irradiance, integrated phytoplankton PP and SAV maximum colonization depth).

4.2. Habitat requirements for SAV: estimating water quality objectives for restoration and preservation

Macrophytes play a central role in modulating ecosystem dynamics, regulating nutrient cycle, influencing food webs structure, controlling trophic status and maintaining a physical habitat complexity of shallow lakes and estuaries. In addition, they play an important role in maintaining biodiversity by providing shelter to a variety of associated organisms (e.g., Orth and Moore, 1983; Scheffer et al., 1994; Jeppesen et al., 1998; Bayley and Prather,

2003). Consequently, many studies, research programs and management efforts have been focused on SAV dynamics. It is important to point out, however, that clear state with SAV is not necessarily the desirable ecosystem state for all shallow lakes. For instance, lakes of different geographic zones have shown peculiarities in ecosystem stability. In addition, alternative primary producers could dominate contrasting states in some systems (Scheffer and van Nes, 2007).

Determination of IOPs, specific absorption and scattering coefficients, in conjunction with Kirk's model could be used to determine target water quality conditions needed to restoration of SAV in these highly turbid lakes. Additionally, managers can consider the most attainable remediation action and determine habitat requirements with different minimum light constraints. In studied lakes, reduction of phytoplankton alone, via nutrient reduction, would not be suitable per se to considerably increase depth limits to SAV developing. Instead, it will be necessary a more integrative action. A radical reduction of 95% of TSS and T-Chl *a* would be needed to increase Z_{SAV} about 0.5 m (representing values of TSS < 13.3 mg L⁻¹ and T-Chl *a* < 24 µg L⁻¹). Value of Z_{SAV} between 0.5 and 1 m would represent important areas of these shallow lakes (maximum depth around 2 m). A relative controllability of TSS, which comes from *in situ* resuspension, can be archived by the construction of refuges to reduce wind and wave activity (Smart and Dick, 1999), compacting sediments via drawdown (Scheffer, 1998) and removing key fish species to control bioturbation (Smith et al., 2001). Target values of TSS and T-Chl *a*, obtained to archive $Z_{SAV} = 0.5$ in these lakes, are lower than that estimated by Gallegos (1994, 2001) and than observed by Dennison et al. (1993) for estuarine waters. This is explained by the higher background attenuation caused by high CDOM absorption coefficients in studied lakes. If we consider for example the values of $a_g(440)$ measured by Gallegos (1994) and a 22% of SAV light requirement, comparable values of water quality parameters were archived for Lake Chascomús (TSS = 20 mg L⁻¹ and T-Chl *a* = 40 µg L⁻¹). Reduction of CDOM concentration would be achieved, for instance, after reduction of suspended particulates, increasing water transparency and promoting photobleaching.

Of course, an array of factors in addition to water column transparency can influence the distribution and abundance of SAV (Koch, 2001; Havens, 2003; Bakker et al., 2013), especially water level, sediment type and light attenuation at the leaf surface by epiphytic algae (Weisner et al., 1997; Gafny and Gasith, 1999; Van Geest et al., 2007). Therefore, it is important to note that Kirk's model predicts only water column attenuation and relates it with optical water quality parameters. This optical model should be viewed as an analytical tool to determinate a benchmark of minimal habitat requirement, in a defined light criterion, to restore or protect SAV.

4.3. Absorptive characteristics of natural phytoplankton populations in highly turbid environments

The evaluation of variation in phytoplankton absorption characteristics (i.e., phytoplankton absorption, phytoplankton specific absorption and spectral matching parameters) is important to accurately estimate phytoplankton PP using bio-optical models, remote estimation of pigment biomass and forecast harmful algal blooms (e.g., Sosik, 1996; Millie et al., 1997; Gons, 1999; Markager and Vincent, 2001). The $a_{ph}^*(\lambda)$ values reported here were found to be within the previously described range (e.g., Bricaud et al., 1995; Suzuki et al., 1998) and were lower than those observed in ultra-oligotrophic waters. Hence, the observed $a_{ph}^*(\lambda)$ values are in agreement with the trophic regime hypothesis (Yentsch and Phinney, 1989). The studied lakes, however, were found to have

higher $a_{ph}^*(440)$ values than those reported for eutrophic ocean waters, which contain much lower Chl *a* concentrations (e.g., Bricaud et al., 1995; Vantrepotte et al., 2007). Comparable values of $a_{ph}^*(440)$ at high Chl *a* concentrations were also observed for the turbid, shallow Lake Taihu (Le et al., 2009; Zhang et al., 2010); therefore, identify potential differences in the interplaying factors affecting phytoplankton absorption properties between eutrophic lakes and oceanic/costal waters. Several studies have shown variation in $a_{ph}^*(\lambda)$ due to either photophysiological acclimation or taxonomical changes within the algal assemblages (e.g., Mitchell and Kiefer, 1988; Bricaud and Stramski, 1990). In turbid waters, light is regarded as one of the main factors regulating phytoplankton growth. In the studied lakes, PAR was attenuated within the first few cm and their spectral compositions were quickly comprised of wavelengths that are poorly absorbed by phytoplankton (i.e., $A_e < 1$). Moreover, assessing the importance of underwater light field on the variation of $a_{ph}^*(\lambda)$ in shallow polymictic lakes is difficult. Within the mixed layer, phytoplankton is subjected to constant irradiance changes. In a recent work carried out in Lake Chascomús, the variation of $a_{ph}^*(\lambda)$ was found to be closely related to changes in the cell pigment content, which was a response to seasonal variation of incident light. In addition, lower values of $a_{ph}^*(\lambda)$ were observed during spring and summer when higher attenuation coefficients and elevated absorption by unpigmented particles were present (Pérez et al., 2011). In the present work, the variation in $a_{ph}^*(\lambda)$ could not be a priori related to differences in either light attenuation or in the mean water column irradiances. Some of the variation in $a_{ph}^*(\text{Blue})$ and $a_{ph}^*(\text{PAR})$, however, were explained by differences in the ratio between unpigmented particulate absorption and phytoplankton absorption. For instance, in Lake La Limpia, much of the light energy was removed from the system by unpigmented particulate absorption and lower values of $a_{ph}^*(\text{Blue})$ and $a_{ph}^*(\text{PAR})$ were observed at high background turbidity. These observations are in agreement with previous findings from Pérez et al. (2011) in Lake Chascomús. Contrastingly, in Lake San Jorge, light limitation is mainly caused by phytoplankton self-shading and higher values of $a_{ph}^*(\text{Blue})$ and $a_{ph}^*(\text{PAR})$ were observed. In this case, the bulk of light energy is effectively incorporated into the pelagic food web. Therefore, this lake can support higher algal biomass with similar values of light attenuation. Furthermore, some of the observed variation in $a_{ph}^*(\text{Blue})$ could be explained with differences in pigment composition among lakes (i.e., differences in TAP/T-Chl *a* ratios). The composition of pigments was in close agreement with the dominance of major algal classes observed for each lake by Allende et al. (2009). The determination of Fucox and Diato in Lakes La Limpia and Chascomús, however, would be only related with presence of diatoms. On the other hand, variations in $a_{ph}^*(\text{Red})$ can be explained by pigment package effect and the interactive action of pigment composition. In the three studied lakes, the package effect reduced the values for $a_{ph}^*(\text{Red})$ by approximately 53% [mean value of $Q_s^*(675) = 0.47$]. Specifically, in Lake Chascomús the presence of Chl *b* counteracts the effect of pigment packaging and explains the observed higher $a_{ph}^*(\text{Red})$ values. Our results on bio-optical properties of phytoplankton showed different responses to the nature of light competition in these high turbidity environments.

5. Conclusions

The current study presents a comprehensive description of optically active substances and optical properties and their interrelationships that illustrate the complexity of turbid lakes. In spite of the good general relationships between $K_d(\text{PAR})$ and common light penetration estimates (i.e., T_n or Z_{SD}) observed in studied lakes, imprecise predictions of light attenuation could be

obtained if either generalised factors are used or lake-specific relationships are not evaluated. In turn, this inaccuracy can translate into potential errors in the determination of some key parameters used in water management, restoration processes and ecosystem monitoring (e.g., estimations of mean water column irradiance, integrated phytoplankton PP and maximum depth of SAV colonization). On the other hand, this study provides empirical support for the use of Kirk's model to estimate K_d (PAR) in turbid lakes. In addition, optical model was used to determine target water quality conditions needed to restoration of SAV. In these lakes an integrative remediation action, considering substantial reduction of TSS, Chl *a* and CDOM, must be contemplated to increase potential habitats for SAV colonization. Managers could use optical properties in conjunction with Kirk's model as a procedure for calculating minimum water quality goals for protection and restoration of SAV in turbid shallow lakes.

Finally, the findings concerning absorptive characteristics of natural phytoplankton populations contribute to a better understanding of microalgae ecophysiology growing under strong light-limited conditions.

Acknowledgements

Financial support was provided by The Argentinean network for the assessment and monitoring of Pampean shallow-lakes (PAMPA²), CONICET (PIP 00700) and ANPCyT (PICT07-429). Thanks to Victor Valenzuela for correcting the manuscript.

Appendix A. Supplementary material

Supplementary material associated with this article can be found, in the online version, at <http://dx.doi.org/10.1016/j.jenvman.2013.09.001>.

References

- Allende, L., Tell, G., Zagarese, H., Torremorell, A., Pérez, G., Bustingorry, J., Escaray, R., Izaguirre, I., 2009. Phytoplankton and primary production in clear-vegetated, inorganic-turbid, and algal-turbid shallow lakes from the pampa plain (Argentina). *Hydrobiologia* 624, 45–60.
- APHA, 1998. Standard Methods for the Examination of Water and Wastewater. American Publication Health Association, Washington DC.
- Bakker, E.S., Sarneel, J.M., Gulati, R.D., Liu, Z., Donk, E., 2013. Restoring macrophyte diversity in shallow temperate lakes: biotic versus abiotic constraints. *Hydrobiologia* 710, 23–37.
- Bayley, S.E., Prather, C.M., 2003. Do wetland lakes exhibit alternative stable states? Submersed aquatic vegetation and chlorophyll in western boreal shallow lakes. *Limnol. Oceanogr.* 48, 2335–2345.
- Belmont, P., Hargreaves, B.R., Morris, D.P., Williamson, C.E., 2007. Estimating attenuation of ultraviolet radiation in streams: field and laboratory methods. *Photochem. Photobiol.* 83, 1339–1347.
- Belzile, C., Vincent, W.F., Kumagai, M., 2002. Contribution of absorption and scattering to the attenuation of UV and photosynthetically available radiation in Lake Biwa. *Limnol. Oceanogr.* 47, 95–107.
- Bricaud, A., Babin, M., Morel, A., Claustre, H., 1995. Variability in the chlorophyll-specific absorption coefficients of natural phytoplankton: analysis and parameterization. *J. Geophys. Res.* 100, 13321–13332.
- Bricaud, A., Stramski, D., 1990. Spectral absorption of living phytoplankton and nonalgal biogenic matter: a comparison between the Peru upwelling area and the Sargasso Sea. *Limnol. Oceanogr.* 35, 562–582.
- Caffrey, A.J., Hoyer, M.V., Canfield, D.E., 2007. Factors affecting the maximum depth of colonization by submersed macrophytes in Florida lakes. *Lake Reservoir Manage.* 23, 287–297.
- Canfield, E.D., Langeland, K.A., Linda, S.B., Haller, W.T., 1985. Relations between water transparency and maximum depth of macrophyte colonization in lakes. *J. Aquat. Plant Manage.* 23, 25–28.
- Chanson, H., Takeuchi, M., Trevethan, M., 2008. Using turbidity and acoustic backscatter intensity as surrogate measures of suspended sediment concentration in a small subtropical estuary. *J. Environ. Manage.* 88, 1406–1416.
- Cleveland, J.S., Weidemann, A.D., 1993. Quantifying absorption by aquatic particles: a multiple scattering correction for glass-fiber filters. *Limnol. Oceanogr.* 38, 1321–1327.
- Davies-Colley, R.J., Smith, D.G., 2001. Turbidity, suspended sediment, and water clarity: a review. *J. Am. Water Resour. Assoc.* 37, 1085–1101.
- Dennison, W.C., Orth, R.J., Moore, K.A., Stevenson, J.C., Carter, V., Kollar, S., Bergstrom, P.W., Batiuk, R.A., 1993. Assessing water quality with submersed aquatic vegetation, habitat requirements as barometers of Chesapeake Bay health. *BioScience* 43, 86–94.
- Effler, S.W., 1985. Attenuation versus transparency. *J. Environ. Eng.* 111, 448–459.
- Ferrero, E., Eöry, M., Ferreyra, G., Schloss, I., Zagarese, H., Vernet, M., Momo, F., 2006. Vertical mixing and ecological effects of ultraviolet radiation in planktonic communities. *Photochem. Photobiol.* 82, 898–902.
- Gafny, S., Gasith, A., 1999. Spatially and temporally sporadic appearance of macrophytes in the littoral zone of Lake Kinneret, Israel: taking advantage of a window of opportunity. *Aquat. Bot.* 62, 249–267.
- Gallegos, C.L., 1994. Refining habitat requirements of submersed aquatic vegetation: role of optical models. *Estuaries* 17, 187–199.
- Gallegos, C.L., 2001. Calculating optical water quality targets to restore and protect submersed aquatic vegetation: overcoming problems in partitioning the diffuse attenuation coefficient for photosynthetically active radiation. *Estuaries* 24, 381–397.
- Gallegos, C.L., Jordan, T.E., Hines, A.H., Weller, D.E., 2005. Temporal variability of optical properties in a shallow, eutrophic estuary: seasonal and interannual variability. *Estuar. Coast. Shelf Sci.* 64, 156–170.
- Gerbeaux, P., Ward, J.C., 1991. Factors affecting water clarity in Lake Ellesmere, New Zealand. *New Zeal. J. Mar. Freshwater Res.* 25, 289–296.
- Gons, H.J., 1999. Optical teledetection of chlorophyll *a* in turbid inland waters. *Environ. Sci. Technol.* 33, 1127–1132.
- Gordon, H.R., Morel, A.Y., 1984. Remote assessment of ocean color for interpretation of satellite visible imagery: a review. *J. Mar. Biol. Assoc. U. K.* 64, 969.
- Guisande, C., Barreiro, A., Acuña, A., Marciales, L.J., Hernández, E., Torres, A.M., Aranguren, N., López, W., Duque, S.R., Gallo, L.J., Aguirre, N., Mogollón, M., Palacio, J., Rueda-Delgado, G., 2008. Testing of the CHEMTAX program in contrasting neotropical lakes, lagoons, and swamps. *Limnol. Oceanogr.* Methods 6, 643–652.
- Hargeby, A., Blindow, I., Andersson, G., 2007. Long-term patterns of shifts between clear and turbid states in lake Krankesjön and lake Takern. *Ecosystems* 10, 29–36.
- Havens, K.E., 2003. Submerged aquatic vegetation correlations with depth and light attenuating materials in a shallow subtropical lake. *Hydrobiologia* 493, 173–186.
- Hobbs, W.O., Ramstack Hobbs, J.M., LaFrancois, T., Zimmer, K.M., Theissen, K.M., Edlund, M.B., Michelutti, N., Butler, M.G., Hanson, M.A., Carlson, T.J., 2012. A 200-year perspective on alternative stable state theory and lake management from a biomanipulated shallow lake. *Ecol. Appl.* 22, 1483–1496.
- Ibelings, B.W., Portielje, R., Lammens, E.H.R.R., Noordhuis, R., Van Den Berg, M.S., Joosse, W., Meijer, M.L., 2007. Resilience of alternative stable states during the recovery of shallow lakes from eutrophication: Lake Veluwe as a case study. *Ecosystems* 10, 4–16.
- Jackson, L.J., 2003. Macrophyte-dominated and turbid states of shallow lakes: evidence from Alberta lakes. *Ecosystems* 6, 213–223.
- Jeppesen, E., Kristensen, P., Jensen, J.P., Søndergaard, M., Mortensen, E., Lauridsen, T., 1991. Recovery resilience following a reduction in external phosphorus loading of shallow, eutrophic Danish lakes: duration, regulating factors and methods for overcoming resilience. *Mem. Ist. Ital. Idrobiol.* 48, 127–148.
- Jeppesen, E., Søndergaard, M., Søndergaard, M., Christoffersen, K., 1998. The Structuring Role of Submerged Macrophytes in Lakes. Springer-Verlag, New York.
- Kagalou, I., Papastergiadou, E., Leonardos, I., 2008. Long term changes in the eutrophication process in a shallow Mediterranean lake ecosystem of W. Greece: response after the reduction of external load. *J. Environ. Manage.* 87, 497–506.
- Kirk, J.T.O., 1981. Monte Carlo study of the nature of the underwater light field in, and the relationships between optical properties of, turbid yellow waters. *Aust. J. Mar. Freshwater Res.* 32, 517–532.
- Kirk, J.T.O., 1984. Dependence of relationship between inherent and apparent optical properties of water on solar altitude. *Limnol. Oceanogr.* 29, 350–356.
- Kirk, J.T.O., 1991. Volume scattering function, average cosines, and the underwater light field. *Limnol. Oceanogr.* 36, 455–467.
- Kirk, J.T.O., 1994a. Light and Photosynthesis in Aquatic Ecosystems, second ed. Cambridge University Press, New York.
- Kirk, J.T.O., 1994b. Characteristics of the light field in highly turbid waters: a Monte Carlo study. *Limnol. Oceanogr.* 39, 702–706.
- Kishino, M., Takahashi, M., Okami, N., 1985. Estimation of the spectral absorption coefficients of phytoplankton in the sea. *Bull. Mar. Sci.* 37, 634–642.
- Koenings, J.P., Edmundson, J.A., 1991. Secchi disk and photometer estimates of light regimes in Alaskan lakes: effects of yellow color and turbidity. *Limnol. Oceanogr.* 36, 91–105.
- Koch, E.W., 2001. Beyond light: physical, geological and geo-chemical parameters as possible submerged aquatic vegetation habitat requirements. *Estuaries* 24, 1–17.
- Kufel, L., Kufel, I., 2002. Chara beds acting as nutrient sinks in shallow lakes – a review. *Aquat. Bot.* 72, 249–260.
- Laurion, I., Lami, A., Sommaruga, R., 2002. Distribution of mycosporine-like amino acids and photoprotective carotenoids among freshwater phytoplankton assemblages. *Aquat. Microb. Ecol.* 26, 283–294.
- Le, C., Li, Y., Zha, Y., Sun, D., 2009. Specific absorption coefficient and the phytoplankton package effect in Lake Taihu, China. *Hydrobiologia* 619, 27–37.

- Markager, S., Vincent, W.F., 2001. Light absorption by phytoplankton: development of matching parameter for algal photosynthesis under different spectral regimes. *J. Plankton Res.* 23, 1373–1384.
- Marra, J., Trees, C.C., O'Reilly, J.E., 2007. Phytoplankton pigment absorption: a strong predictor of primary productivity in the surface ocean. *Deep Sea Res. I: Oceanogr. Res. Papers* 54, 155–163.
- Middelboe, A.L., Markager, S., 1997. Depth limits and minimum light requirements of freshwater macrophytes. *Freshwater Biol.* 37, 553–568.
- Millie, D.F., Scholfield, O.M., Kirkpatrick, G.J., Johnsen, G., Tester, P.A., Vinyard, B.T., 1997. Detection of harmful algal blooms using photopigments and absorption signatures: a case study of the Florida red tide dinoflagellate, *Gymnodinium breve*. *Limnol. Oceanogr.* 42, 1240–1251.
- Mitchell, B.G., Bricaud, A., Carder, K.L., Cleveland, J.S., Ferrari, G.M., Gould, R., et al., 2000. Determination of spectral absorption coefficients of particles, dissolved material and phytoplankton for discrete water samples. In: Fargion, G.S., Mueller, J.L., McClain, C.R. (Eds.), *Ocean Optics Protocols for Satellite Ocean Color Sensor Validation, Revision 2*. NASA, Maryland, pp. 125–153.
- Mitchell, B.G., Kiefer, D.A., 1988. Chlorophyll a specific absorption and fluorescence excitation spectra for light-limited phytoplankton. *Deep Sea Res.* 35, 639–663.
- Morel, A., 1978. Available, usable, and stored radiant energy in relation to marine photosynthesis. *Deep Sea Res.* 25, 673–688.
- Morel, A., Gentili, B., 1991. Diffuse reflectance of oceanic waters: its dependence on sun angle as influenced by the molecular scattering contribution. *Appl. Opt.* 30, 4427–4438.
- Nolen, S.L., Wilhm, J., Howick, G., 1985. Factors influencing inorganic turbidity in a great plains reservoir. *Hydrobiologia* 123, 109–117.
- Orth, R.J., Moore, K.A., 1983. Chesapeake Bay: an unprecedented decline in submerged aquatic vegetation. *Science* 222, 51–53.
- Padial, A.A., Thomaz, S.M., 2008. Prediction of the light attenuation coefficient through the Secchi disk depth: empirical modeling in two large Neotropical ecosystems. *Limnology* 9, 143–151.
- Pérez, G.L., Llames, M.E., Lagomarsino, L., Zagarese, H., 2011. Seasonal variability of optical properties in a highly turbid lake (Laguna Chascomús, Argentina). *Photochem. Photobiol.* 87, 659–670.
- Pérez, G.L., Torremorell, A., Bustingorry, J., Escaray, R., Pérez, P., Diéguez, M., Zagarese, H., 2010. Optical characteristics of shallow lakes from the Pampa and Patagonia regions of Argentina. *Limnologia* 40, 30–39.
- Poole, H.H., Atkins, W.R.G., 1929. Photo-electric measurements of submarine illumination throughout the year. *J. Mar. Biol. Assoc. U. K.* 16, 297–324.
- Pope, R.M., Fry, E.S., 1997. Absorption spectrum (380–700 nm) of pure water. II. Integrating cavity measurements. *Appl. Opt.* 36, 8710–8723.
- Quirós, R., Boveri, M.B., Petrachi, C.A., Renella, A.M., Rosso, J.J., Sosnovsky, A., von Bernard, H.T., 2006. Los efectos de la agriculturización del humedal pampeano sobre la eutrofización de sus lagunas. In: Tundizi, J.G., Matsumura-Tundisi, T., Sidagis Galli, C. (Eds.), *Eutrofização na América do Sul: Causas, conseqüências e tecnologias de gerenciamento e controle*. IIE, pp. 1–16.
- Quirós, R., Renella, A.M., Boveri, M.B., Rosso, J.J., Sosnovsky, A., 2002. Factores que afectan la estructura y el funcionamiento de las lagunas pampeanas. *Ecol. Austral* 12, 175–185.
- Scheffer, M., Hosper, S.H., Meijer, M.L., Moss, B., Jeppesen, E., 1993. Alternative equilibria in shallow lakes. *Trends Ecol. Evol.* 8, 275–279.
- Scheffer, M., Van den Berg, M., Breukelaar, A., Breukers, C., Coops, H., Doef, R., Meijer, M.L., 1994. Vegetated areas with clear water in turbid shallow lakes. *Aquat. Bot.* 49, 193–196.
- Scheffer, M., 1998. *Ecology of Shallow Lakes*. Chapman & Hall, London.
- Scheffer, M., van Nes, E.H., 2007. Shallow lakes theory revisited: various alternative regimes driven by climate, nutrients, depth and lake size. *Hydrobiologia* 584, 455–466.
- Schwarz, A.M., de Winton, M., Hawes, I., 2002. Species-specific depth zonation in New Zealand charophytes as a function of light availability. *Aquat. Bot.* 72, 209–217.
- Sosik, H., 1996. Bio-optical modeling of primary production: consequences of variability in quantum yield and specific absorption. *Mar. Ecol. Prog. Ser.* 143, 225–238.
- Smart, R.M., Dick, G.O., 1999. *Propagation and Establishment of Aquatic Plants: a Handbook for Ecosystem Restoration Projects*. Technical Report A-99-4. U.S. Army Engineer Waterways Experiment Station, Vicksburg, MS.
- Smith, T., Lundholm, J., Simser, L., 2001. Wetland vegetation monitoring in Cootes paradise: measuring the response to a fishway/carp barrier. *Ecol. Restor.* 19, 145–154.
- Strömbeck, N., Pierson, D.C., 2001. The effects of variability in the inherent optical properties on estimations of chlorophyll a by remote sensing in Swedish freshwaters. *Sci. Total Environ.* 268, 123–137.
- Suzuki, K., Kishino, M., Sasaoka, K., Saitoh, S., Saina, T., 1998. Chlorophyll-specific absorption coefficients and pigment of phytoplankton off Sanriku, North-western North Pacific. *J. Oceanogr.* 54, 517–526.
- Tassan, S., Ferrari, G.M., 1995. An alternative approach to absorption measurements of aquatic particles retained on filters. *Limnol. Oceanogr.* 40, 1358–1368.
- Tassan, S., Ferrari, G.M., 1998. Measurement of light absorption by aquatic particles retained on filters: determination of the optical pathlength amplification by the transmittance-reflectance method. *J. Plankton Res.* 20, 1699–1709.
- Tegler, B., Sharp, M., Johnson, M., 2001. Ecological monitoring and assessment network's proposed core monitoring variables: an early warning of environmental change. *Environ. Monit. Assess.* 67, 29–55.
- V-Balogh, K., Németh, B., Vörös, L., 2009. Specific attenuation coefficients of optically active substances and their contribution to the underwater ultraviolet and visible light climate in shallow lakes and ponds. *Hydrobiologia* 632, 91–105.
- Van Geest, G.J., Coops, H., Scheffer, M., van Nes, E.H., Long, 2007. Transients near the ghost of a stable state in eutrophic shallow lakes with fluctuating water levels. *Ecosystems* 10, 37–47.
- Vantrepotte, V., Brunet, C., Mériaux, X., Lécuyer, E., Vellucci, V., Santer, R., 2007. Bio-optical properties of coastal waters in the Eastern English Channel. *Estuar. Coast. Shelf Sci.* 72, 201–212.
- Weisner, S.E.B., Strand, J.A., Sandsten, H., 1997. Mechanisms regulating abundance of submerged vegetation in shallow eutrophic lakes. *Oecologia* 109, 592–599.
- Yentsch, C.S., Phinney, D.A., 1989. A bridge between ocean optics and microbial ecology. *Limnol. Oceanogr.* 34, 1694–1705.
- Zhang, Y., Qin, B., Zhu, G., Zhang, L., Yang, L., 2007a. Chromophoric dissolved organic matter (CDOM) absorption characteristics in relation to fluorescence in Lake Taihu, China, a large shallow subtropical lake. *Hydrobiologia* 581, 43–52.
- Zhang, Y., Zhang, B., Ma, R., Feng, S., Le, C., 2007b. Optically active substances and their contributions to the underwater light climate in Lake Taihu, a large shallow lake in China. *Fundam. Appl. Limnol.* 170, 11–19.
- Zhang, Y., Feng, L., Li, J., Luo, L., Yin, Y., Liu, M., Li, Y., 2010. Seasonal-spatial variation and remote sensing of phytoplankton absorption in Lake Taihu, a large eutrophic and shallow lake in China. *J. Plankton Res.* 32, 1023–1037.
- Zhang, Y., Liu, X., Yin, Y., Wang, M., Qin, B., 2012. Predicting the light attenuation coefficient through Secchi disk depth and beam attenuation coefficient in a large, shallow, freshwater lake. *Hydrobiologia* 693, 29–37.